

Fig. 3 Mass transfer for $P_T = 1.0$ atm, $S = 0.7$.

gime is shown by a vertical, solid line. This was determined from mass-loss data supplied by a manufacturer of BN at 1.0 atm and with low-velocity air flow. It simply represents the temperature at which the weight-loss curve increases rapidly with temperature. The location of this point relative to the B_2O_3 saturation curve in Fig. 2 indicates a major part may be played by the oxide in protecting the surface at the lower temperatures, since the rate regime was determined from experimental data at 1.0 atm. Increasing the Schmidt number from 0.5 to 0.7, greatly reduced the effect of the weighting factor U_L/U_E on the mass-transfer parameter.

The heat transfer is presented in terms of a parameter, $-2\dot{q}_s/\rho_e u_e C_f$, as a function of wall temperature. Under the sign convention adopted, the negative value of the parameter is the heat that must be supplied to the wall to maintain the wall temperature. The heat-transfer calculations do not consider the possible condensation of B_2O_3 or boron. For the heat-transfer data presented here, the freestream temperature was taken as 537°R, and the kinetic-energy term in the enthalpy difference was neglected. The results are given in Fig. 4 for two pressures, 0.01 and 1.0 atm, two values of the weighting factor U_L/U_E , and for $P = 0.8$ and $S = 0.5$. The

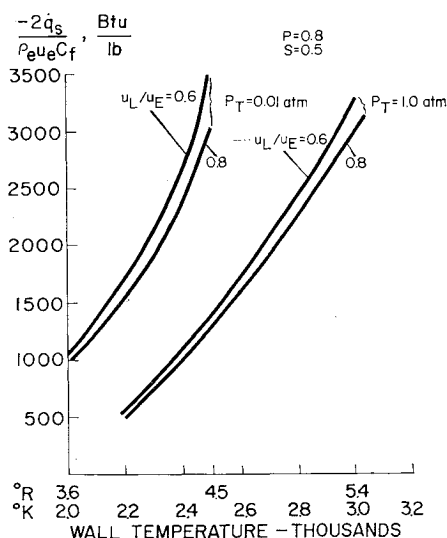


Fig. 4 Heat-transfer parameter for $P_T = 0.01$ and 1.0 atm, $P = 0.8$, and $S = 0.5$.

relatively high slopes of these curves result from a decreasing contribution to the heat-transfer parameter from combustion and an increase in the decomposition rate with increasing wall temperature.

References

- ¹ Kotlensky, W. V. and Martens, H. E., "Tensile behavior of pyrolytic boron nitride to 2200°C," *Nature* 196, 1090-1091 (1962).
- ² Litz, L. M. and Mercuri, R. A., "Oxidation of boron carbide by air, water and air-water mixtures at elevated temperatures," *J. Electrochem. Soc.* 110, 921-925 (1963).
- ³ Powers, D. J., "Static oxidation tests on boron nitride and on a titanium diboride-boron nitride composition," Bell Lab. Rept. 62-14(M), Revision A., Bell Aerosystems Co. (Oct. 1962).
- ⁴ Bowen, M. D. and Gorton, C. W., "The combustion of pyrolytic boron nitride," *AIAA Progress in Astronautics and Aeronautics; Heterogeneous Combustion*, edited by H. G. Wolfhard, I. Glassman, and L. Green, Jr. (Academic Press, New York, 1961), Vol. 15, pp. 251-278.
- ⁵ Lees, L., *Combustion and Propulsion, Third AGARD Colloquium* (Pergamon Press, New York, 1959), pp. 451-498.
- ⁶ McBride, B. J., Heimerl, S., Ehlers, J. G., and Gordon, S., "Thermodynamic properties to 6000°K for 210 substances involving the first 18 elements," NASA SP-3001 (1963).
- ⁷ Dorrance, W. H., *Viscous Hypersonic Flow* (McGraw-Hill Book Company, Inc., 1962), pp. 206-242.

Specular and Lambert Reflection Problems in Radiation Dynamics

STEPHEN N. FALKEN* AND CHENG-TING HSU†
Iowa State University, Ames, Iowa

I. Introduction

IN space that is free of the gravitational and geomagnetic fields of celestial bodies, vehicles will still experience external forces such as those due to solar radiation. For space missions requiring precise trajectory control, the effects of these external forces must be accounted for. Cotter¹ and Dugan² have surveyed the dynamics of solar sails under the condition of specular reflection. Specular reflection is a simple, mirror-like reflection, which corresponds to no interaction between the radiation and the surface. Another simple reflection, which does not require a model used for interaction, is the Lambert reflection. The Lambert process, which diffusely reflects the incident radiation uniformly in all directions, contrasts with the specular process as two rather extreme limits in reflection processes. The present note aims to compare the dynamic effects on bodies due to these two limiting cases. The lift and drag coefficient of a flat plate, a circular cylinder, and a sphere in a parallel, incident radiation field will be evaluated for comparison.

II. Dynamic Forces in a Radiation Field

The energy and momentum contained in a volume V of an electromagnetic field in empty space may be written in gaus-

Received September 28, 1964; revision received March 29, 1965. This research was supported by the Iowa Engineering Experiment Station.

* Research Associate, Engineering Experiment Station and graduate student, Department of Aerospace Engineering; now member of technical staff, Aerospace Corporation, San Bernardino, Calif.

† Professor, Department of Aerospace Engineering and Engineering Experiment Station. Member AIAA.

sian mixed units as³

$$U = (1/8\pi) \int (E^2 + H^2) dV \quad (1)$$

$$\bar{m} = (1/4\pi c) \int (\bar{E} \times \bar{H}) dV \quad (2)$$

respectively. The electric-field strength, magnetic-field intensity, and speed of light are denoted by \bar{E} , \bar{H} , and c , respectively. In this case, \bar{E} and \bar{H} are orthogonal and of equal magnitude.³ Equations (1) and (2) are related by

$$\bar{m} = (U/c) \bar{r} \quad (3)$$

where \bar{r} is a unit vector in the direction of the wave propagation. It follows that the radiation force exerted per unit area of a surface element $d\sigma$ is

$$\bar{f} = \lim_{d\sigma, dt \rightarrow 0} [(1/c)(dU/d\sigma dt) \bar{r}] \quad (4)$$

The integrated intensity of radiation over the entire frequency spectrum for parallel, incident beams on $d\sigma$ may be defined as

$$I_0 = \lim_{d\sigma, dt \rightarrow 0} (dU/d\sigma \cos\theta_0 dt) \quad (5)$$

where θ_0 is the acute angle between the direction of incident rays and the inward normal from the surface $d\sigma$ as shown in Fig. 1. The integrated intensity of diffusely reflected radiation from $d\sigma$ over the entire frequency spectrum is defined⁴ as

$$I_r(\theta, \phi) = \lim_{d\sigma, dt, d\omega \rightarrow 0} (dU/d\sigma \cos\theta dt d\omega) \quad (6)$$

where θ is the acute angle between the direction of reflected rays and the outward normal \bar{n} from $d\sigma$. $d\omega = \sin\theta d\theta d\phi$ is a small solid angle pointing at an arbitrary direction from $d\sigma$. Thus, in terms of the intensities, the radiation force per unit area may be written as

$$\bar{f}_0 = (I_0/c) \cos\theta_0 \bar{r}(\theta', \phi) \quad (7)$$

for parallel, incident rays, and

$$\bar{f}_r = (1/c) \iint I_r(\theta, \phi) \bar{r}(\theta', \phi) \sin\theta \cos\theta d\theta d\phi \quad (8)$$

for diffusely reflected rays. In Eqs. (7) and (8), the unit vector

$$\bar{r}(\theta', \phi) = \bar{i} \cos\theta' + \bar{j} \sin\theta' \sin\phi + \bar{k} \sin\theta' \cos\phi \quad (9)$$

is referred to the rectangular coordinates x , y , and z as shown in Fig. 1. Note that $\theta' = \theta_0$ is an acute angle for parallel incident rays and that $\theta' = \pi - \theta$ is an obtuse angle for reflected rays. Resolving these radiation forces along each of the rectangular coordinates, respectively, one obtains the radiation pressure and shear from Eq. (7), for parallel, incident rays,

$$p_0 = (I_0/c) \cos^2\theta_0 \quad (10a)$$

$$(\tau_{xy})_0 = (I_0/c) \cos\theta_0 \sin\theta_0 \sin\phi_0 \quad (10b)$$

$$(\tau_{xz})_0 = (I_0/c) \cos\theta_0 \sin\theta_0 \cos\phi_0 \quad (10c)$$

and from Eq. (8), for diffusely reflected rays,

$$p_r = \frac{1}{c} \int_0^{2\pi} \int_0^{\pi/2} I_r(\theta, \phi) \cos^2\theta \sin\theta d\theta d\phi \quad (11a)$$

$$(\tau_{xy})_r = \frac{1}{c} \int_0^{2\pi} \int_0^{\pi/2} I_r(\theta, \phi) \cos\theta \sin^2\theta \sin\phi d\theta d\phi \quad (11b)$$

$$(\tau_{xz})_r = \frac{1}{c} \int_0^{2\pi} \int_0^{\pi/2} I_r(\theta, \phi) \cos\theta \sin^2\theta \cos\phi d\theta d\phi \quad (11c)$$

where the integration limits of $\theta = 0$ to $\pi/2$ and $\phi = 0$ to 2π have been inserted. In the preceding discussion, the interaction between the incident and reflected rays has been neglected, since the cross section for the scattering of light by

light is extremely small^{5,6} in the absence of external fields. The total pressure and shear acting on $d\sigma$ and resulting from all the incident and reflected rays may be expressed in forms as, for example, in free molecule flow theory

$$p_t = p_0 + p_r \quad \tau_t = \tau_0 + \tau_r \quad (12)$$

where the subscripts 0, r , and t denote the parallel incident, reflected, and total values, respectively.

Now consider a surface element $d\sigma$ of an arbitrary body shape in Fig. 1. Let the incident rays be parallel to the x - y plane with $\phi_0 = \pi/2$ and make an angle of attack[†] α with the inward surface normal. The lift and drag forces acting on $d\sigma$, defined in the directions normal and parallel to the incident rays, respectively, may be expressed in terms of p_t and τ_t as follows:

$$dF_L = (p_t \sin\alpha - \tau_t \cos\alpha) d\sigma \quad (13)$$

$$dF_D = (p_t \cos\alpha + \tau_t \sin\alpha) d\sigma \quad (14)$$

1. Specular reflection

The reflected intensity is related to the incident one by $I_r = \lambda I_0$ with $\theta_r = \theta_0$ and $\phi_r = \phi_0$. λ is known as the "albedo" or momentum reflectivity. The reflected pressure and shear, in this case, follow the relationship of Eq. (10) and are related to the incident ones by

$$p_r = (I_r/c) \cos^2\theta_r = (\lambda I_0/c) \cos^2\theta_0 = \lambda p_0 \quad (15)$$

$$\tau_r = (I_r/c) \cos\theta_r \sin\theta_r = (\lambda I_0/c) \cos\theta_0 \sin\theta_0 = \lambda \tau_0 \quad (16)$$

The total pressure and shear from Eq. (12), with $\theta_0 = \alpha$, are

$$p_t(\alpha, \lambda) = (1 + \lambda)(I_0/c) \cos^2\alpha \quad (17)$$

$$\tau_t(\alpha, \lambda) = (1 - \lambda)(I_0/c) \cos\alpha \sin\alpha \quad (18)$$

Substitution of Eqs. (17) and (18) into Eqs. (13) and (14) yields, respectively, the lift and drag on $d\sigma$

$$dF_L = (I_0/c) 2\lambda \cos^2\alpha \sin\alpha d\sigma \quad (19)$$

$$dF_D = (I_0/c) (1 + \lambda \cos 2\alpha) \cos\alpha d\sigma \quad (20)$$

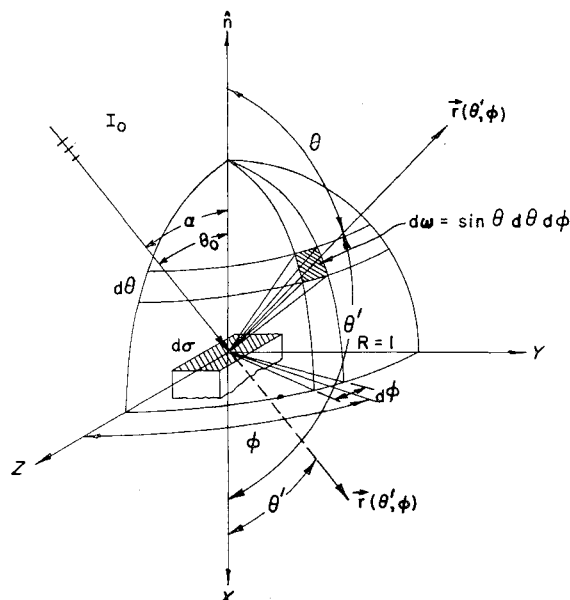


Fig. 1 Spherical coordinate system in a radiation field.

† Note that $\alpha = \theta_0$ is defined herein in accordance with the convention of the incident angle θ_0 in radiation theory and differs from that in conventional aerodynamics which is simply $\pi/2 - \alpha$.

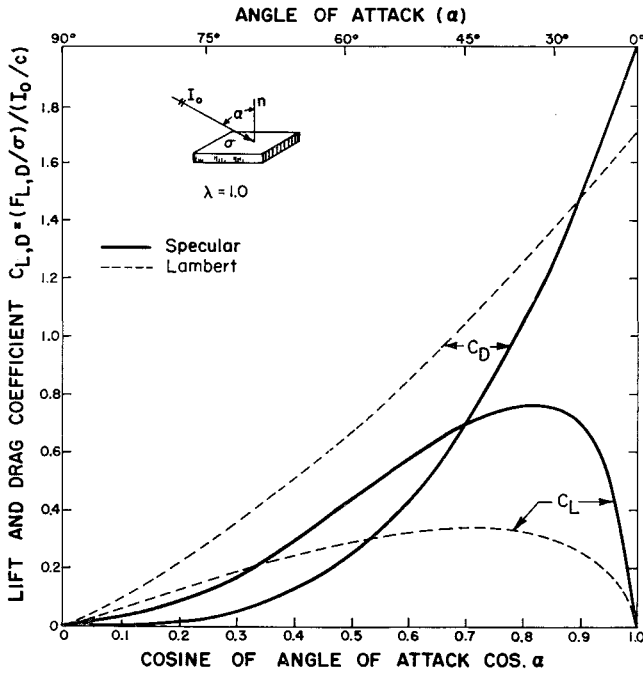


Fig. 2 Lift and drag coefficients of a flat plate for perfectly specular and Lambert reflection.

2. Lambert reflection

The diffusely reflected intensity is taken to be a constant in all directions and is related⁴ with the incident intensity by $I_r = (\lambda I_0 \cos \alpha) / \pi$. Substitution of I_r into Eqs. (11) yields

$$p_r = (2\lambda I_0 \cos \alpha) / 3c \quad (\tau_{xy})_r = (\tau_{xz})_r = 0 \quad (21)$$

In a similar manner, one obtains

$$p_r(\alpha, \lambda) = (I_0/c) \cos \alpha [\cos \alpha + \frac{2}{3}\lambda] \quad (22)$$

$$\tau_x(\alpha) = (I_0/c) \cos \alpha \sin \alpha \quad (23)$$

$$dF_L = (2I_0/3c)\lambda \cos \alpha \sin \alpha d\sigma \quad (24)$$

$$dF_D = (I_0/c) \cos \alpha [1 + \frac{2}{3}\lambda \cos \alpha] d\sigma \quad (25)$$

III. Application to Several Body Shapes

Since the incident radiation always impacts on a moving body with the relative velocity of light because of relativistic consideration,³ α remains constant despite the motion of the body.

Flat plate

Defining the lift and drag coefficient as $C_{L,D} = (F_{L,D}/\sigma) / (I_0/c)$ where σ is the flat-plate area, one obtains C_L and C_D from Eqs. (19, 20, 24, and 25) for the following reflection processes:

Specular

$$C_L(\alpha, \lambda) = \lambda \sin 2\alpha \cos \alpha \quad (26)$$

$$C_D(\alpha, \lambda) = (1 + \lambda \cos 2\alpha) \cos \alpha \quad (27)$$

Lambert

$$C_L(\alpha, \lambda) = \frac{1}{3}\lambda \sin 2\alpha \quad (28)$$

$$C_D(\alpha, \lambda) = [1 + \frac{2}{3}\lambda \cos \alpha] \cos \alpha \quad (29)$$

Equations (26–29) are plotted in Fig. 2 for $\lambda = 1$. Although the lift and drag coefficients are linearly proportional to the momentum reflectivity λ , the specular reflection shows more angular dependence of α than the Lambert reflection. Since the incident pressure is the same for both reflection processes, and the ratio of the reflected pressure for the specular case to the Lambert case is $\frac{2}{3} \cos \alpha$, the total pressure is higher in

the specular case than in the Lambert case for $\alpha < 48.2^\circ$, and vice versa. In addition, the total shear is always larger for the Lambert case than for the specular case. These facts together with the relationship expressed in Eqs. (13) and (14) account for the lift and drag distribution shown in Fig. 2. The drag coefficient for the Lambert case always increases with λ for any $\alpha < 90^\circ$, whereas, for the specular case, it increases with λ for $\alpha < 45^\circ$ but decreases with increase in λ for $\alpha > 45^\circ$ as seen in Eq. (27). However, the drag coefficient decreases with increase in α for both reflection processes. At $\alpha = 90^\circ$, $C_D = 0$ for both processes since, for radiation to exert a force, the radiative energy flux must be able to hit on a surface. In the conventional sense, it may be interpreted that radiation rays are frictionless.

Circular cylinder

The incident rays are considered in the direction perpendicular to the longitudinal axis (i.e., z axis) of the right circular cylinder and are making variable angles of attack with the inward normal (i.e., x axis) of the surface element. The surface element $d\sigma$, in this case, may be written as $R d\alpha dz$, where R is the radius of the circular cylinder. Defining C_L and C_D as $(F_{L,D}/2RL) / (I_0/c)$, where L is the length of cylinder, and performing the integration for Eqs. (19, 20, 24, and 25) with the limit of $\alpha = -90^\circ$ to $+90^\circ$ and $z = 0$ to L , one obtains the following results:

Specular

$$C_L = 0 \quad C_D(\lambda) = 1 + (\lambda/3) \quad (30)$$

Lambert

$$C_L = 0 \quad C_D(\lambda) = 1 + (\pi\lambda/6) \quad (31)$$

The drag coefficients increase linearly with λ , but the Lambert reflection exhibits higher drag than the specular case for a given λ . It is because the resultant of the reflected Lambert force always acts normally toward the body surface and results in a reflected C_D of $\pi\lambda/6$, whereas the specularly reflected force may occur in a direction that reduces the drag of the cylinder for $\alpha > 45^\circ$.

Sphere

Because of the axially symmetric property in this case, the area element $d\sigma$ under consideration may be taken as a ring-shaped strip. The area of this strip is $2\pi R \sin \alpha \cdot R d\alpha$, where R is the radius of the sphere. Defining C_L and C_D as $(F_{L,D}/\pi R^2) / (I_0/c)$ and performing the integration for Eqs. (19, 20, 24, and 25) with the limit of $\alpha = 0^\circ$ to 90° , one obtains

Specular

$$C_L = 0 \quad C_D = 1 \quad (32)$$

Lambert

$$C_L = 0 \quad C_D(\lambda) = 1 + (4\lambda/9) \quad (33)$$

For specular reflection on a sphere, the reflected rays are directed in such a manner that the net effect cancels out. The drag in this case is due to the incident radiation only and is, of course, independent of the momentum reflectivity λ . However, there is additional drag besides the incident one in the Lambert case. This additional C_D , which results from the Lambert reflected pressure, is equal to $4\lambda/9$ as shown in Eq. (33).

References

- 1 Cotter, T. P., "Solar sailing," Sandia Corporation Rept. SCR-78 (1959).
- 2 Dugan, D. W., "A preliminary study of a solar-probe mission," NASA TN D-783 (1961).
- 3 Richtmyer, F. K., Kennard, E. H., and Lauritsen, T., *Introduction to Modern Physics* (McGraw-Hill Book Co., Inc., New York, 1955), 5th ed., Appendix I, pp. 633–635 and Chap. II, p. 61.

⁴ Chandrasekhar, S., *Radiative Transfer* (Oxford University Press, Oxford, England, 1950), Chap. I, pp. 1-2 and Chap. VI, p. 147.

⁵ McKenna, J. and Platzman, P. M., "Nonlinear interaction of light in a vacuum," *Phys. Rev.* **129**, 2354-2360 (1963).

⁶ Jauch, J. M. and Rohrlich, F., *Theory of Photons and Electrons* (Addison-Wesley Publishing Co., Inc., Reading, Mass., 1955), pp. 287-296.

Determination of Hot-Gas Temperature Profiles from Infrared Emission and Absorption Spectra

BURTON KRAKOW*

Warner and Swasey Company, Flushing, N. Y.

I. Introduction

WE have studied the relationships between the temperature distribution in a hot gas and the infrared emission and absorption spectra of the gas, with a view to determining gas temperature profiles from line-of-sight spectral measurements. Temperature gradients affect the exchange of radiant energy between different regions of a hot gas and, consequently, affect the observed spectra. As a result, it is possible to obtain information about the temperature distribution in a hot gas from a study of its emission and absorption spectra.

II. Theory

Emittance equations

When temperature gradients exist in a gas, it is possible to consider the gas to consist of a series of zones, each of which is isothermal within the precision of measurement. If the gradients are steep the regions would have to be small, but, in principle, such a division always can be made. If we number these zones serially from 1 to n , with zone 1 nearest the detector, the irradiance of the detector, $H(\lambda_i)$, by monochromatic radiation of wavelength λ_j , is given¹ by Eq. (1)

$$H(\lambda_j) = \sum_{i=1}^n W_b(\lambda_j, T_i) [1 - \tau_i(\lambda_j)] \prod_{h=0}^{i-1} \tau_h(\lambda_j) \quad (1)$$

$W_b(\lambda_j, T_i)$ is the Planck function at wavelength λ_j and the temperature T_i of zone i . $\tau_i(\lambda_j)$ denotes the transmittance of zone i at λ_j . The right side of Eq. (1) is simply the emittance of each zone i , as given by Kirchhoff's Law, multiplied by the transmittance of the gas between zone i and the detector, summed over all of the zones. For monochromatic radiation, the transmittance of any number of zones is the product of the transmittances of the component zones. Zone zero is the medium between the sample and the detector.

In practice, the measured radiant energy is never truly monochromatic. Over the finite slit width $\Delta\lambda'$ of the monochromator used, the Planck function usually can be considered constant, but this is not true of the transmittance of a gas. If $g(\lambda_j, \lambda')$ symbolizes the spectrometer slit function at λ_j , and measured quantities are labeled by a subscript m ,

we can write

$$\begin{aligned} H_m(\lambda_j) &= \int_{\Delta\lambda'} H(\lambda') g(\lambda_j, \lambda') d\lambda' \\ &= \sum_{i=1}^n W_{bm}(\lambda_j, T_i) [\bar{\tau}_{(i-1)}(\lambda_j) - \bar{\tau}_i(\lambda_j)] \end{aligned} \quad (2)$$

where

$$\bar{\tau}_i(\lambda_j) = \frac{\int_{\Delta\lambda'} \prod_{h=0}^i \tau_h(\lambda') g(\lambda_j, \lambda') d\lambda'}{\int_{\Delta\lambda'} g(\lambda_j, \lambda') d\lambda'} \quad (3)$$

Physically, $\bar{\tau}_i(\lambda_j)$ is the transmittance of the section of the sample, composed of zones 0- i , that would be measured at λ_j with the slit function $g(\lambda_j, \lambda')$ and a spectral slit width $\Delta\lambda'$, and $W_{bm}(\lambda_j, T_i)$ is the spectral emittance of a blackbody at T_i that would be measured at λ_j with a slit function $g(\lambda_j, \lambda')$ and a spectral slit width $\Delta\lambda'$. Since the blackbody emittance is effectively constant over the values of $\Delta\lambda'$ corresponding to practical slit widths, $W_{bm}(\lambda_j, T_i)$ can be separated into two factors, one of which is independent of temperature, and the other is independent of slit function. Thus

$$W_{bm}(\lambda_j, T_i) = W_b(\lambda_j, T_i) \int_{\Delta\lambda'} g(\lambda_j, \lambda') d\lambda' \quad (4)$$

Since $W_b(\lambda_j, T_i)$ is given by the Planck law, a measurement of the apparent emittance $W_{bm}(\lambda_j, T_b)$ of a blackbody at any convenient temperature T_b can be used to evaluate

$$\int_{\Delta\lambda'} g(\lambda_j, \lambda') d\lambda'$$

Then, when Eq. (2) is solved for the values of $W_{bm}(\lambda_j, T_i)$, the temperatures can be obtained from the corresponding values of $W_b(\lambda_j, T_i)$, and the results will be independent of the slit function.

For an isothermal temperature profile, $n = 1$, and Eq. (2) therefore contains only one transmittance $\bar{\tau}(\lambda_j)$, provided that the optical path outside the hot-gas sample is free of absorbing gas, i.e., the path is evacuated or flushed with a nonabsorbing gas so that $\bar{\tau}_0(\lambda_j) = 1$. Moreover, $\bar{\tau}(\lambda_j)$ can be measured directly, as can $H_m(\lambda_j)$. Equation (2) then reduces to

$$H_m(\lambda_j) = W_{bm}(\lambda_j, T) [1 - \bar{\tau}(\lambda_j)] \quad (2a)$$

Equation (2a) has the form of Kirchhoff's law. It can be solved for the only remaining variable $W_{bm}(\lambda_j, T)$ from which the temperature can be determined. This is the infrared brightness method of temperature measurement.² If Eq. (2a) is applied to a nonisothermal system, the wavelength-dependent result is a weighted average of the temperatures in the sample.

In applying Eq. (2) to a nonisothermal temperature profile, spectral emittance is measured at n different wavelengths, having n different sets of values of $\bar{\tau}_i(\lambda_j)$. This yields n independent simultaneous equations for calculating the n temperatures.

The infrared transmittances that appear in Eq. (2) are themselves somewhat temperature-dependent. Moreover, of the n transmittances that must be obtained, only one $[\bar{\tau}_n(\lambda_j)]$ can be measured directly. Therefore, solution of Eq. (2) requires some a priori knowledge of the transmittances of the molecular species comprising the hot-gas specimen, particularly a knowledge of how they vary with temperature. This knowledge may take the form of empirical data, theoretical formulas, or a combination of these. Once such information is available, our system of irradiance equations can be solved for the thermal structure of the specimen. We have developed and tested the following iterative procedure for carrying out this solution.

Presented as Preprint 65-105 at the AIAA 2nd Aerospace Sciences Meeting, New York, N. Y., January 25-27, 1965; revision received March 31, 1965. This work was supported by the Air Force Office of Scientific Research. The author would like to thank R. H. Tourin for his assistance in this work.

* Senior Physicist, Control Instrument Division.